Published in final edited form as:
Bone. 2012 November ; 51(5): 868–875. doi:10.1016/j.bone.2012.08.124.

Increased Variability of Bone Tissue Mineral Density Resulting from Estrogen Deficiency Influences Creep Behavior in a Rat Vertebral Body

Do-Gyoon Kim[a,*], **Anand R. Navalgund**[a], **Boon Ching Tee**[a], **Garrett J. Noble**[b], **Richard T. Hart**[b], and **Hye Ri Lee**[a]

[a]Division of Orthodontics, College of Dentistry, The Ohio State University, Columbus, OH 43210, USA

[b]Department of Biomedical Engineering, College of Engineering, The Ohio State University, Columbus, OH 43210, USA

Abstract

Progressive vertebral deformation increases the fracture risk of a vertebral body in the postmenopausal patient. Many studies have observed that bone can demonstrate creep behavior, defined as continued time-dependent deformation even when mechanical loading is held constant. Creep is a characteristic of viscoelastic behavior, which is common in biological materials. We hypothesized that estrogen deficiency-dependent alteration of the mineral distribution of bone at the tissue level could influence the progressive postmenopausal vertebral deformity that is observed as the creep response at the organ level. The objective of this study was thus to examine whether the creep behavior of vertebral bone is changed by estrogen deficiency, and to determine which bone property parameters are responsible for the creep response of vertebral bone at physiological loading levels using an ovariectomized (OVX) rat model. Correlations of creep parameters with bone mineral density (BMD), tissue mineral density (TMD) and architectural parameters of both OVX and sham surgery vertebral bone were tested. As the vertebral creep was not fully recovered during the post-creep unloading period, there was substantial residual displacement for both the sham and OVX groups. A strong positive correlation between loading creep and residual displacement was found ($r=0.868$, $p<0.001$). Of the various parameters studied, TMD variability was the parameter that best predicted the creep behavior of the OVX group ($p<0.038$). The current results indicated that creep caused progressive, permanent reduction in vertebral height for both the sham and OVX groups. In addition, estrogen deficiency-induced active bone remodeling increased variability of trabecular TMD in the OVX group. Taken together, these results suggest that increased variability of trabecular TMD resulting from high bone turnover influence creep behavior of the OVX vertebrae.

[*]For correspondence, Do-Gyoon Kim, Ph.D., Assistant Professor, Division of Orthodontics, College of Dentistry, The Ohio State University, 4088 Postle Hall, 305 W. 12th Ave, Columbus, OH 43210, USA, kim.2508@osu.edu, Tel) (614) 247-8089, Fax) (614) 688-3077.

Keywords

Viscoelastic creep; Ovariectomized rat; Estrogen deficiency; Tissue mineral density; Vertebral deformation

Introduction

One quarter of postmenopausal women are expected to have at least one osteoporotic vertebral compression fracture in their lifetime [1–3]. Vertebral deformity is considered to be responsible for about half of the age-related vertebral fractures that occur during daily activities [4, 5]. Observations have shown that the risk of vertebral deformity was significantly higher in postmenopausal osteoporotic patients than in healthy people [6]. It was also observed that progressive vertebral deformation could lead to vertebral fractures [7, 8]. However, the detailed mechanism of how long-term vertebral deformation accumulates has not been fully understood.

The vertebra is a load-bearing organ that sustains the constant load of body weight. This prolonged constant loading on vertebral bone could produce creep, which is a time-dependent continuous deformation observed in viscoelastic materials under a constant load [9]. Many studies have examined the creep behavior of cortical bone [10–13], cancellous bone [14–16], and animal and human vertebral bodies [4, 17, 18] under either fatigue or constant long-term loading. It was observed that creep propagated even at physiological levels of loading for human vertebral bone [15–17]. The developed creep was not fully recovered by post-creep unloading, resulting in a permanent residual deformation. Thus, it is reasonable to speculate that accumulation of residual deformation could lead to the progressive development of vertebral deformity. However, the etiology of residual deformation of a vertebral body remains unclear.

Bone mineral density (BMD) and architecture have been widely examined to help estimate the mechanical properties of bone [19]. While BMD and bone architecture showed strong positive correlations with the elastic and fracture properties of bone, they were not able to explain the viscoelastic creep of bone [15, 17]. On the other hand, it was suggested that tissue mineral density (TMD) is another important parameter that can influence the mechanical properties of bone [20]. While BMD is defined as the mineral content within an apparent volume of bone, including porosity and bone marrow as well as bone matrix, TMD represents the mineral content only in the hard tissue of bone [21]. A recent study found that variability of TMD could account for the creep response of human vertebral trabecular bone to a small compressive loading [16]. It was also shown that the TMD variability of postmenopausal osteoporotic bone increased as a result of estrogen deficiency-induced active bone remodeling [22, 23]. Together, these findings suggest that the creep behavior of bone is likely altered following the change in TMD variability that occurs with postmenopause. However, no study has been performed to investigate the relationship between altered TMD distribution and the viscoelastic creep behavior of postmenopausal vertebral bone.

In the current study, we hypothesized that estrogen deficiency-dependent alteration of the mineral distribution at the tissue level could influence the progressive postmenopausal vertebral deformity that is observed as the creep response at the organ level. Thus, the objective of this study was to examine whether the creep behavior of vertebral bone is changed by estrogen deficiency, and to determine which bone property parameters are responsible for the creep response of vertebral bone at physiological loading levels using an

OVX rat model. The parameters to be examined were BMD, TMD and the architectural parameters of rat vertebral bone.

Materials and Methods

Specimen preparation

Following an experimental protocol approved by the Institutional Animal Care and Use Committee (IACUC) of The Ohio State University, two groups of Sprague-Dawley female rats (6 months old, 288±24 g) were obtained from Harlan Sprague Dawley, Inc. (Indianapolis, IN). One rat group received a bilateral ovariectomy (OVX) operation and the other group received a sham operation. After an 8-week post-operation period, the rats were euthanized and vertebrae were obtained. After the removal of all soft tissue and posterior processes, the vertebral specimens were stored at −21°C until utilization.

Micro-computerized tomography

After thawing at room temperature, specimens were scanned by a micro-computerized tomography (micro-CT) scanner (SkyScan 1172-D, Kontich, Belgium) with the scanning and reconstruction voxel sizes set at 16×16×16 μm^3. The same scanning conditions (49 kV, 200 μA, 0.4° rotation per projection, 8 frames averaged per projection, and 40 ms exposure time) were used for all specimens. Using a calibration curve based on known density phantoms scanned under the same micro-CT conditions, the CT attenuation value of each bone voxel was converted to the tissue mineral density (TMD) of bone, as introduced in a previous study [24]. Non-bone voxels outside the vertebral cortex were cleaned using a heuristic algorithm [25], while all voxels inside the vertebral cortex were maintained (Fig. 1). The entire three-dimensional (3D) region of vertebral centrum was masked using a compartmentalizing method that we modified based on a procedure used in a previous study to isolate a region of femoral trabecular bone [26]. After bone voxels inside each vertebral image were segmented from non-bone voxels using the heuristic algorithm, bone voxels of the vertebral cortex (CB) were digitally separated from those of the trabecular bone (TB) in the centrum using the masked image of the vertebral centrum (Fig. 1). All of the masking and compartmentalizing steps were performed using Image J software (NIH).

The masked volume represented the total volume (TV) of TB (Fig. 1). Bone mineral density (BMD) was calculated by dividing the sum of TB TMD by TV. Mean value (Mean) of TMD was computed by dividing the sum of TMD values by the total number of voxels in each region using the TMD histograms of TB and CB (Fig. 2). Variability of TMD was represented by the standard deviation (SD) and coefficient of variation (COV), which was computed by dividing the SD by the Mean. Low and high TMD (Low and High) were determined at the lower and upper 5th percentile values, respectively (Fig.2b). Total TB fraction (BV/TV) was obtained by calculating the volume ratio of TB to TV. In addition, TB architectural parameters were measured in the largest possible cylindrical region of interest (ROI) in the vertebral centrum. The volume of the ROI was the same for all specimens. Commercial micro-CT software (Microview, GE) was used to compute trabecular surface-to-volume ratio (BS/BV), thickness (Tb.Th), number (Tb.N), separation (Tb.Sp), and connectivity density (Conn.D) as defined in a previous study [25].

Creep test

Following micro-CT scanning, creep tests were performed using a commercial loading device (ELF 3230, Bose, MN) with a 450 N load cell. An environmental chamber system installed on the loading machine was used to control temperature (37°C) and maintain specimen moisture during the creep tests. The solution used was 0.9% normal saline with 57.5 mg/l Ca^{++} to prevent mineral dissolution during long-term creep testing, as suggested

in a previous study [27]. Before mechanical testing, machine compliance was measured following a procedure from a previous study [28] and later taken into account in the calculation of creep displacements. The height of each vertebra was measured using the micro-CT image. Each isolated vertebral body was aligned in the loading cups following a procedure that was used in a previous study for compressive mechanical testing of whole human vertebral bodies [29]. Dental cement was mixed with water until it reached a doughy stage. A small portion of the doughy dental cement was placed into the loading cup. Next, the vertebral specimen was placed into the doughy dental cement of one loading cup and aligned in the craniocaudal direction. We ensured that the bone cement covered the entire endplate of the vertebra. Before the dental cement was completely cured, the position of the vertebral body was adjusted so that the surface of its endplate was parallel to the loading cup. The loading cup with the vertebral body was mounted on the upper axis of the loading machine. The other loading cup containing the doughy dental cement was mounted on the lower axis of the loading machine. The vertebral specimen potted in the upper loading cup was lowered, by operating the loading machine, until the entire surface of the opposite endplate was covered by the doughy bone cement in the lower loading cup. The vertebral specimen was kept hydrated while the bone cement cured. The initial compressive stiffness of each bone specimen was determined by applying 10 pre-cycles of a small apparent strain (2000 με) to each rat vertebra under displacement control. All displacement data were obtained using a high-resolution (15 nm) displacement transducer, which was integrated with the loading machine. After the pre-cyclic loading, all other mechanical tests were performed under load control. The specimens were compressed at a load level corresponding to a randomly assigned initial static apparent strain level, set at 2377.5±1226.4 με, for both the sham and OVX groups. This strain range was determined to be comparable to the peak physiological compressive strain of bone, which is in the range of 2100 to 3100 με, as measured and estimated in previous studies [30, 31]. After determining the physiological initial static apparent strain level, the applied initial static displacement was estimated by multiplying the strain by the vertebral height. As a result, the applied initial displacement levels were estimated to be 0.016±0.009 mm in the current study, which was about 5% of the yield displacement (over 0.3 mm) of a rat lumbar vertebra measured in a previous study [32]. Finally, the applied initial static load value, consistent with the estimated initial static displacement, was computed by multiplying the initial static displacement and the initial stiffness as estimated during the pre-loading cycles. Loads were applied at a rate that corresponded to a strain rate of 0.01 ε/sec. Following 2-hour compressive creep loading, each specimen was fully unloaded at the same loading rate and allowed to recover for 2 hours (Fig. 4). The durations of the loading-unloading cycles were the same as those used for the creep tests performed on whole human vertebral bodies in a previous study [17]. The applied static displacement (d_j), corresponding to the applied static load (f_j), was measured during loading. The variable d_j represents the elastic displacement of a specimen under the physiological loading. Loading creep (C_j) was computed by subtracting the initial displacement from the displacement measured at the end of 2 hours of creep loading. The variable C_j accounts for the gradual displacement of a specimen under the prolonged, constant, and physiological constant loading. Unloading creep recovery (C_{ul}) was obtained by subtracting the final displacement (residual displacement (d_{res})) at the end of the 2-hour unloading process from the displacement measured at the end of the static unloading. During the process of static unloading, while each specimen was still contained within the loading pot of the machine, the creep loading on the specimen was released. Then, C_{ul} was measured as the gradual displacement of each specimen during the 2-hour holding period following the static unloading process. Although the displacement of each specimen was partially recovered upon unloading, it was not fully recovered, leaving the residual displacement, d_{res}. The creep parameters were normalized to the applied static displacements (d_j) to compare the creep response under a uniform displacement condition between specimens.

Statistical Analysis

Of the total number of lumbar vertebrae (41) obtained from 36 rats, 15 vertebrae were not available for analysis due to data acquisition errors. This experimental error rate was comparable to that of previous fatigue-creep experimental studies [4, 33]. Excluding those specimens, the creep data from 26 lumbar vertebrae (9 L3, 9 L4 and 8 L5) from 24 rats (12 rats for each group) were analyzed. As one vertebra from each rat was used, with the exception of one rat from each group from which two vertebrae were obtained, data from 13 vertebrae from each group were successfully analyzed in the current study. Analysis of variance (ANOVA) was performed to compare data between the sham and OVX groups for BMD, TMD (TB_{Mean}, TB_{SD}, TB_{COV}, TB_{low}, TB_{high}, CB_{Mean}, CB_{SD}, CB_{COV}, CB_{low}, CB_{high}), TB architectural parameters (BV/TV, Tb.N, Tb.Th, Tb.Sp, BS/BV, and Conn.D), the initial conditions of the creep test (f_i and d_i), creep (C_l, C_{ul}, d_{res}) and the normalized creep (C_l/d_i, C_{ul}/d_i, d_{res}/d_i) parameters. For each group, Pearson's correlation coefficients were used to examine correlations between creep parameters and between normalized creep parameters. If significant correlations were found for both groups, analysis of covariance (ANCOVA) was used to test whether the correlations were different between the two groups. To identify the parameter that best explained the vertebral creep behavior, stepwise regressions were performed when comparisons of the creep parameters and the normalized creep parameters with BMD, TMD and the architectural parameters were significantly different between the sham and OVX groups. Significance was set at $p<0.05$ for all statistical tests.

Results

The BMD and TB TMD parameters were significantly higher for the sham group than for the OVX group ($p<0.021$), except for TB_{SD} and TB_{COV}, which were significantly lower for the sham group than for the OVX group ($p<0.05$) (Table 1). While CB_{mean} and CB_{low} were significantly higher for the sham group than for the OVX group ($p<0.016$), CB_{SD}, CB_{COV} and CB_{high} were not significantly different between the two groups ($p>0.232$). The TB bone volume fraction (BV/TV) and thickness (Tb.Th) were significantly higher for the sham group than for the OVX group ($p<0.002$), but the surface-to-volume ratio of bone (BS/BV) was significant lower for the sham group than for the OVX group ($p<0.002$). Other TB architectural parameters were not significantly different between the two groups ($p>0.140$).

Original vertebral height was not significantly different between the sham (6.720±0.223 mm) and OVX (6.666±0.341 mm) groups ($p=0.635$). The creep test initial condition parameters (applied load and displacement) were not significantly different between the two groups ($p>0.136$, Table 1). A substantial loading creep was observed in both groups under the constant physiological loading conditions over 2 hours (Fig. 4). Total vertebral deformation, caused by the combination of initial static displacement and creep, was not fully recovered during the 2 hour unloading duration, resulting in a substantial residual displacement for both groups. None of the creep parameters were significantly different between the two groups ($p>0.619$).

For correlations between the creep parameters, the loading creep had significant correlations with residual displacement for both the sham and OVX groups ($p<0.005$), while other correlations were not significant for both groups ($p>0.335$). The correlations between creep and residual displacement were not significantly different between the two groups (ANCOVA, $p=0.435$). The correlation between creep and residual displacement for all of the vertebrae (sham and OVX) was significantly positive ($r=0.735$, $p<0.001$). Correlations between the normalized creep parameters followed the same trends as the creep parameters. The only significant correlation was between normalized creep and residual displacement

for both groups (Fig. 5, r=0.868, p<0.001 for the pooled groups), while no other correlations were significant (p>0.06).

The stepwise regression indicated that BV/TV had the best positive correlation with loading creep for the sham group (p=0.05), and that TB_{SD} had a strong negative correlation with the unloading creep recovery for the OVX group (p<0.001) (Table 2 and Fig. 6). When the creep parameters were normalized with applied displacement (d_l), BMD and CB_{low} had the best positive correlations with normalized loading creep and residual displacement, respectively, for the sham group (p<0.043) (Table 2). For the OVX group, TMD variability (TB_{SD} and TB_{COV}) was the parameter with the best positive correlation with normalized loading creep and residual displacement (p<0.038), and a negative correlation with normalized unloading creep recovery (p<0.023). The TB_{SD} had a strong positive correlation with TB_{COV} for both groups (r=0.925, p<0.001).

Discussion

The observed time-dependent vertebral deformation was not fully recovered during the post-creep unloading period, resulting in substantial residual displacement (d_{res}) for both the sham and OVX groups. The strong positive correlation between loading creep (C_l) and d_{res} indicated that the creep caused by prolonged loading at a modest elastic level could give rise to the progressive permanent reduction in vertebral height for both groups. The TMD variability was the parameter that best determined the unloading creep recovery (C_{ul}) and the normalized creep parameters (C_l/d_l, C_{ul}/d_l, d_{res}/d_l) for the OVX group. It was observed that higher rates of trabecular bone turnover due to active bone remodeling amplify the variability of TB TMD in an OVX rat model [22, 34]. Taken together, these results suggest that an increase in the variability of TB TMD resulting from high bone turnover plays an important role in controlling the viscoelastic creep behavior of the OVX rat vertebrae.

Estrogen deficiency has been shown to stimulate excessive osteoclast resorption activities in an OVX rat model [22, 35]. An imbalance between bone resorption and formation can cause a net loss of bone tissue, resulting in a lower bone mass (BMD and BV/TV) in the OVX rat group when compared to the control rat group [22, 35, 36]. Consistent with the previous results, we found that TB BMD and BV/TV of the OVX group were lower than they were in the sham group. To be sure these parameters were measured based on the entire region of vertebral cancellous centrum, we isolated the centrum by following the digital separation between the vertebral centrum and the vertebral cortex in the 3D micro-CT images (Fig. 1). Thus, the current results should provide a comprehensive analysis that avoids a potential measurement bias due to the regional variation of trabecular bone mass in the vertebral centrum [37, 38].

Recently, it was found that creep had a significant positive correlation with post-creep residual deformation in human vertebral cancellous bone after a constant physiological level of loading [16]. In the current study, we also found that substantial creep development was significantly correlated with the permanent residual deformation of the vertebrae in both the sham and OVX rat groups. This result indicated that creep is responsible for the progressive accumulation of permanent damage in vertebrae during long-term loading at the relatively modest physiological level.

Bone mass parameters have been accepted as strong surrogates for stiffness and strength of bone [19, 39]. Because creep is a time-dependent deformation that continues with constant loading, we speculated that creep would be reduced by increasing the bone mass parameters. However, contrary to our expectations, the amount of creep increased with increasing BV/TV and BMD for the sham group. Furthermore, these bone mass parameters did not account

for changes in other creep parameters in either the sham or OVX group. Yamamoto et al. [15] indicated that there was no significant correlation between apparent density and creep in human vertebral cancellous bone. Pollintine et al. [17] also observed no significant correlation between BMD and the anterior wedge angle (deformation) of a human vertebral body during creep loading. Their results suggested that the mechanism involved in controlling the viscoelastic creep behavior of bone is different from that involved in the elastic and fracture response of bone. Thus, new parameters, other than the traditional parameters that have been used to explain the elastic and fracture properties of bone, are needed to describe the viscoelastic creep behavior of a whole vertebra.

Previous studies suggested that the trabecular architecture of vertebral centrum could affect the mechanical properties of vertebral bone [22, 40]. The trabecular thickness (Tb.Th) and fracture strength of rat vertebrae were shown to have significantly decreased 2 months post-OVX, while trabecular formation and resorption surface area were increased [22]. In the current study, we also observed that Tb.Th decreased and BS/BV increased 2 months after OVX, but the viscoelastic creep parameters did not change in association with those architectural parameters. Brouwers et al. [4] found no correlation between centrum trabecular architecture and fatigue-creep development in rat vertebrae. In addition, architectural variation did not explain continuous creep in human vertebral trabecular bone [16]. Taken together, these results indicated that the bone architecture-dependent mechanism involved in static fracture is not applicable to the explanation of the long-term viscoelastic deformation of vertebrae.

It has been thought that bone quality plays an important role in determining the mechanical stability of bone, as well as the overall bone quantity [41]. Bone quantity can be estimated by the bone mass parameters (BV/TV and BMD). On the other hand, the distribution of the TMD parameters, which is a result of bone turnover at different time points, can reflect one of the many different aspects of bone quality [42, 43]. Bone remodeling removes pre-existing (more mineralized) bone tissue while adding immature (less mineralized) bone tissue, and the long-term process of mineralization of the newly formed tissue is started [43]. As such, TMD variability inherently increases while the overall amount of TMD decreases under active bone remodeling. Estrogen deficiency accelerated this process of bone turnover, which is commonly observed in both human and animal bone [22, 23, 34, 43, 44]. Consistent with previous results, we found that TB TMD variability (TB_{SD} and TB_{COV}) was significantly higher in the OVX group than in the sham group, while the parameters of TB TMD (TB_{Mean}, TB_{low}, and TB_{high}) were lower. On the other hand, the CB variability was not significantly different between the two groups, while some parameters of CB TMD (CB_{Mean} and CB_{low}) were significantly lower in the OVX group. These findings indicate that the active bone remodeling triggered by OVX had a greater effect on the TB component of the vertebrae than the CB component by significantly increasing both new bone formation in regions of low mineralization (TB_{low}) and pre-existing bone resorption in highly mineralized regions (TB_{high}) in the OVX TB. Consequently, the TB TMD histogram for the OVX group moved toward lower values than the histogram for the sham group (Fig. 2b). The higher bone turnover rate in the trabecular bone could arise from the fact that the surface area to be remodeled is larger than that in the cortical bone region, as indicated in previous studies [21, 45].

The TB TMD variability was the parameter that controlled the creep parameters. As significant correlations were found only in the OVX group and not in the sham group, it is clear that estrogen deficiency-induced alteration of TB TMD variability has an effect on the creep behavior of an entire OVX vertebra. In order to account for the creep behavior of individual specimens, the creep parameters were normalized via the applied static initial displacement. This uniform displacement condition allows for identification of the roles of

the bone tissue properties in determining the mechanical response of bone, independent of structural variation between specimens [4]. Based on the normalized creep parameters, we found that the increased TB TMD variability of the OVX vertebrae resulted in more permanent residual displacement as a result of the combination of increasing creep and decreasing post-creep recovery. Taken together, the current results suggested that the creep behavior at the organ level of an OVX vertebra could be controlled by the degree of mineral distribution at the tissue level, which is altered by estrogen deficiency-induced active bone remodeling.

The exact mechanism of the creep behavior of bone associated with physiological loading levels has not been clearly understood. Nanoindentation tests on bone tissue showed that more creep occurred in newly forming (less mineralized) bone tissue than in old pre-existing (more mineralized) bone tissue [46]. As such, overall creep at the organ level increases when regions of newly forming bone tissue are added. On the other hand, the TMD-dependent creep development may produce shear movement between adjacent tissues with different mineral densities [47]. If these local micromotions at the tissue level of bone are not fully recovered by unloading, the permanent residual displacement will accumulate with time. The current results reflected these concepts because the creep and residual displacement both increased with increasing TB TMD variability in the OVX group. However, the creep parameters were not significantly different between the sham and OVX groups. We performed an additional analysis to test the correlations between TB TMD variability and the creep parameters of a pooled group, which included both the sham and OVX groups. The same trend of significant correlations was obtained for the pooled group ($p<0.037$) as was found for the OVX group, while the correlation coefficients became weaker when compared to those from the OVX group alone. These results indicate that the creep behavior of the sham group was, in general, controlled by the TMD variability, while some outliers did not follow this trend. Based on these results, we hypothesize that additional creep will develop with further increases in TMD variability resulting from the continued progression of estrogen-deficient postmenopausal osteoporosis in the OVX group, while creep will not continue to develop in the sham group without the estrogen deficiency-induced changes in TMD variability. This additional creep may result in more cumulative post-creep vertebral deformation, which would eventually become distinguishable from what occurs in the sham group. Further studies that include visualization of creep development at the tissue surface are necessary to test this hypothesis.

There are limitations to the current study. First, the vertebral structure of the rat model is not identical to that of human vertebrae. The OVX rat vertebral model has been most commonly used for controlled estrogen deficiency-dependent osteoporosis research [48]. Many previous static and dynamic mechanical tests were performed using OVX rat vertebrae [4, 18, 22]. However, the differences in vertebral structure between rats and humans may give rise to a different distribution of the amount of stress in the bone. It was observed that the variation of trabecular architecture did not influence the creep behavior of human vertebral trabecular bone [16], just as we found using the current rat model. Thus, while the current results were limited to a comparison of the absolute magnitude of the creep parameters to a human vertebral model, it was possible to examine the role of TMD distribution in controlling the creep behavior of bone, independent of its architecture. The second limitation of this study was that creep data from some of the vertebrae were excluded because of the detection of an unstable displacement signal during the prolonged creep period. This data acquisition error may have arisen from a micro-slipping motion at the mechanical interlocking interface between the dental cement and the irregular endplate surface of each rat vertebra. The high-resolution displacement transducer, with a resolution of 15 nm, was able to detect this minute variation in the displacement signal. Thus, only the creep data with a smooth creep curve were included in the current results. Third, we did not attempt to

analyze microcrack development in the bone matrix. Microcracks may have occurred in the current animal vertebral specimens, as it has been observed in human cortical bone under creep as a result of the physiological cyclic loading [49]. In addition, we did not analyze the collagen component of the bone, which has been widely accepted as a key element in determining the viscoelasticity of bone [50, 51]. Recently, Sasaki et al [52] found that the dissolution of mineral from bone reduces its elastic modulus and changes its viscoelastic properties. Furthermore, Pathak et al [53] found a higher viscoelastic response occurred in bone matrix that had a lower mineral-to-matrix ratio. These findings suggest that the viscoelastic properties of bone are likely controlled by a combination of the mineral and collagen components in the bone matrix. We focused on examining the mineral density distribution at the tissue level, so histological analysis of microcracks and the collagen component of the bone matrix were beyond the scope of the current study. If the microcrack and collagen component analyses could be performed on the post-creep vertebral specimens, in combination with the current tissue mineral analysis, it would help to further elucidate the mechanism of the creep behavior of bone.

In conclusion, variability of trabecular tissue mineral density influences the viscoelastic creep behavior of an OVX rat vertebra under long-term compressive loading at the physiological level. It is well known that estrogen deficiency-induced active bone remodeling changes bone mass and architecture, decreasing the elastic and fracture mechanical properties of postmenopausal osteoporotic bone. In addition, we suggest that the distribution of tissue mineralization, which accounts for bone quality, should be considered in the assessment of the time-dependent mechanical response of osteoporotic bone. The current results provide an insight into how bone quality contributes to the accumulation of residual deformation following prolonged compressive creep, which, through aging, is an active process of postmenopausal, osteoporotic vertebral body deformity.

Acknowledgments

The project described here was supported by Grant Number AG033714 from the National Institute on Aging (Kim, D-G). Its contents are solely the responsibility of the authors and do not necessarily represent the official views of the National Institute on Aging.

References

1. Kim DH, Vaccaro AR. Osteoporotic compression fractures of the spine; current options and considerations for treatment. Spine J. 2006; 6:479–487. [PubMed: 16934715]
2. Melton LJ 3rd, Kallmes DF. Epidemiology of vertebral fractures: implications for vertebral augmentation. Acad Radiol. 2006; 13:538–545. [PubMed: 16627192]
3. Melton LJ 3rd, Kan SH, Frye MA, Wahner HW, O'allon WM, Riggs BL. Epidemiology of vertebral fractures in women. Am J Epidemiol. 1989; 129:1000–1011. [PubMed: 2784934]
4. Brouwers JE, Ruchelsman M, Rietbergen B, Bouxsein ML. Determination of rat vertebral bone compressive fatigue properties in untreated intact rats and zoledronic-acid-treated, ovariectomized rats. Osteoporos Int. 2009; 20:1377–1384. [PubMed: 19066708]
5. Riggs BL, Melton LJ 3rd. The worldwide problem of osteoporosis: insights afforded by epidemiology. Bone. 1995; 17:505S–511S. [PubMed: 8573428]
6. Diacinti D, Acca M, D'Erasmo E, Tomei E, Mazzuoli GF. Aging changes in vertebral morphometry. Calcif Tissue Int. 1995; 57:426–429. [PubMed: 8581874]
7. Sone T, Tomomitsu T, Miyake M, Takeda N, Fukunaga M. Age-related changes in vertebral height ratios and vertebral fracture. Osteoporos Int. 1997; 7:113–118. [PubMed: 9166390]
8. Keller TS, Harrison DE, Colloca CJ, Harrison DD, Janik TJ. Prediction of osteoporotic spinal deformity. Spine (Phila Pa 1976). 2003; 28:455–462. [PubMed: 12616157]
9. Lakes, RS. Viscoelastic Solid. New York: CRC Press; 1999. p. 267

10. Caler WE, Carter DR. Bone creep-fatigue damage accumulation. J Biomech. 1989; 22:625–635. [PubMed: 2808445]
11. Cotton, J.; Zioupos, P.; Winwood, K.; Taylor, M. Creep formulation of strain accumulation during tensile fatigue of cortical bone. Proceedings of IV World Congress Biomechanics; Calgary, Canada. 2002. p. 5165
12. Lynch JA, Silva MJ. In vivo static creep loading of the rat forelimb reduces ulnar structural properties at time-zero and induces damage-dependent woven bone formation. Bone. 2008; 42:942–949. [PubMed: 18295561]
13. Rimnac CM, Petko AA, Santner TJ, Wright TM. The effect of temperature, stress and microstructure on the creep of compact bovine bone. J Biomech. 1993; 26:219–228. [PubMed: 8468335]
14. Bowman SM, Keaveny TM, Gibson LJ, Hayes WC, McMahon TA. Compressive creep behavior of bovine trabecular bone. J Biomech. 1994; 27:301–310. [PubMed: 8051190]
15. Yamamoto E, Paul Crawford R, Chan DD, Keaveny TM. Development of residual strains in human vertebral trabecular bone after prolonged static and cyclic loading at low load levels. J Biomech. 2006; 39:1812–1818. [PubMed: 16038915]
16. Kim DG, Shertok D, Ching Tee B, Yeni YN. Variability of tissue mineral density can determine physiological creep of human vertebral cancellous bone. J Biomech. 2011; 44:1660–1665. [PubMed: 21481880]
17. Pollintine P, Luo J, Offa-Jones B, Dolan P, Adams MA. Bone creep can cause progressive vertebral deformity. Bone. 2009; 45:466–472. [PubMed: 19465166]
18. Kummari SR, Davis AJ, Vega LA, Ahn N, Cassinelli EH, Hernandez CJ. Trabecular microfracture precedes cortical shell failure in the rat caudal vertebra under cyclic overloading. Calcif Tissue Int. 2009; 85:127–133. [PubMed: 19488669]
19. Morgan EF, Bayraktar HH, Keaveny TM. Trabecular bone modulus-density relationships depend on anatomic site. J Biomech. 2003; 36:897–904. [PubMed: 12757797]
20. Follet H, Boivin G, Rumelhart C, Meunier PJ. The degree of mineralization is a determinant of bone strength: a study on human calcanei. Bone. 2004; 34:783–789. [PubMed: 15121009]
21. Renders GA, Mulder L, van Ruijven LJ, van Eijden TM. Degree and distribution of mineralization in the human mandibular condyle. Calcif Tissue Int. 2006; 79:190–196. [PubMed: 16969595]
22. Yao W, Cheng Z, Koester KJ, Ager JW, Balooch M, Pham A, Chefo S, Busse C, Ritchie RO, Lane NE. The degree of bone mineralization is maintained with single intravenous bisphosphonates in aged estrogen-deficient rats and is a strong predictor of bone strength. Bone. 2007; 41:804–812. [PubMed: 17825637]
23. Busse B, Hahn M, Soltau M, Zustin J, Puschel K, Duda GN, Amling M. Increased calcium content and inhomogeneity of mineralization render bone toughness in osteoporosis: mineralization, morphology and biomechanics of human single trabeculae. Bone. 2009; 45:1034–1043. [PubMed: 19679206]
24. Mulder L, Koolstra JH, Van Eijden TM. Accuracy of microCT in the quantitative determination of the degree and distribution of mineralization in developing bone. Acta Radiol. 2004; 45:769–777. [PubMed: 15624521]
25. Kim DG, Christopherson GT, Dong XN, Fyhrie DP, Yeni YN. The effect of microcomputed tomography scanning and reconstruction voxel size on the accuracy of stereological measurements in human cancellous bone. Bone. 2004; 35:1375–1382. [PubMed: 15589219]
26. Buie HR, Campbell GM, Klinck RJ, MacNeil JA, Boyd SK. Automatic segmentation of cortical and trabecular compartments based on a dual threshold technique for in vivo micro-CT bone analysis. Bone. 2007; 41:505–515. [PubMed: 17693147]
27. Gustafson MB, Martin RB, Gibson V, Storms DH, Stover SM, Gibeling J, Griffin L. Calcium buffering is required to maintain bone stiffness in saline solution. J Biomech. 1996; 29:1191–1194. [PubMed: 8872276]
28. Kalidindi S, Abusafieh A, ElDanaf E. Accurate characterization of machine compliance for simple compression testing. Experimental Mechanics. 1997; 37:210–215.

29. Kim DG, Dong XN, Cao T, Baker KC, Shaffer RR, Fyhrie DP, Yeni YN. Evaluation of filler materials used for uniform load distribution at boundaries during structural biomechanical testing of whole vertebrae. J Biomech Eng. 2006; 128:161–165. [PubMed: 16532630]
30. Rubin CT, Lanyon LE. Limb mechanics as a function of speed and gait: a study of functional strains in the radius and tibia of horse and dog. J Exp Biol. 1982; 101:187–211. [PubMed: 7166694]
31. Kopperdahl DL, Keaveny TM. Yield strain behavior of trabecular bone. J Biomech. 1998; 31:601–608. [PubMed: 9796682]
32. Barak MM, Weiner S, Shahar R. The contribution of trabecular bone to the stiffness and strength of rat lumbar vertebrae. Spine (Phila Pa 1976). 2010; 35:E1153–E1159. [PubMed: 20881656]
33. Bowman SM, Guo XE, Cheng DW, Keaveny TM, Gibson LJ, Hayes WC, McMahon TA. Creep contributes to the fatigue behavior of bovine trabecular bone. J Biomech Eng. 1998; 120:647–654. [PubMed: 10412444]
34. Ames MS, Hong S, Lee HR, Fields HW, Johnston WM, Kim DG. Estrogen deficiency increases variability of tissue mineral density of alveolar bone surrounding teeth. Arch Oral Biol. 2010; 55:599–605. [PubMed: 20541742]
35. Francisco JI, Yu Y, Oliver RA, Walsh WR. Relationship between age, skeletal site, and time post-ovariectomy on bone mineral and trabecular microarchitecture in rats. J Orthop Res. 2011; 29:189–196. [PubMed: 20722002]
36. Gasser JA, Ingold P, Venturiere A, Shen V, Green JR. Long-term protective effects of zoledronic acid on cancellous and cortical bone in the ovariectomized rat. J Bone Miner Res. 2008; 23:544–551. [PubMed: 18072878]
37. Kim DG, Hunt CA, Zauel R, Fyhrie DP, Yeni YN. The effect of regional variations of the trabecular bone properties on the compressive strength of human vertebral bodies. Ann Biomed Eng. 2007; 35:1907–1913. [PubMed: 17690983]
38. Hulme PA, Boyd SK, Ferguson SJ. Regional variation in vertebral bone morphology and its contribution to vertebral fracture strength. Bone. 2007; 41:946–957. [PubMed: 17913613]
39. Keaveny TM, Hayes WC. A 20-year perspective on the mechanical properties of trabecular bone. J Biomech Eng. 1993; 115:534–542. [PubMed: 8302037]
40. Parkinson IH, Badiei A, Stauber M, Codrington J, Muller R, Fazzalari NL. Vertebral body bone strength: the contribution of individual trabecular element morphology. Osteoporos Int. 2012; 23:1957–1965. [PubMed: 22086309]
41. Hernandez CJ, Keaveny TM. A biomechanical perspective on bone quality. Bone. 2006; 39:1173–1181. [PubMed: 16876493]
42. Roschger P, Gupta HS, Berzlanovich A, Ittner G, Dempster DW, Fratzl P, Cosman F, Parisien M, Lindsay R, Nieves JW, Klaushofer K. Constant mineralization density distribution in cancellous human bone. Bone. 2003; 32:316–323. [PubMed: 12667560]
43. Ruffoni D, Fratzl P, Roschger P, Klaushofer K, Weinkamer R. The bone mineralization density distribution as a fingerprint of the mineralization process. Bone. 2007; 40:1308–1319. [PubMed: 17337263]
44. Roschger P, Paschalis EP, Fratzl P, Klaushofer K. Bone mineralization density distribution in health and disease. Bone. 2008; 42:456–466. [PubMed: 18096457]
45. Allen MR, Turek JJ, Phipps RJ, Burr DB. Greater magnitude of turnover suppression occurs earlier after treatment initiation with risedronate than alendronate. Bone. 2011; 49:128–132. [PubMed: 20637914]
46. Kim DG, Huja SS, Lee HR, Tee BC, Hueni S. Relationships of viscosity with contact hardness and modulus of bone matrix measured by nanoindentation. J Biomech Eng. 2010; 132:024502. [PubMed: 20370248]
47. Jager I, Fratzl P. Mineralized collagen fibrils: a mechanical model with a staggered arrangement of mineral particles. Biophys J. 2000; 79:1737–1746. [PubMed: 11023882]
48. Lelovas PP, Xanthos TT, Thoma SE, Lyritis GP, Dontas IA. The laboratory rat as an animal model for osteoporosis research. Comp Med. 2008; 58:424–430. [PubMed: 19004367]
49. George WT, Vashishth D. Damage mechanisms and failure modes of cortical bone under components of physiological loading. J Orthop Res. 2005; 23:1047–1053. [PubMed: 16140189]

50. Sasaki N, Nakayama Y, Yoshikawa M, Enyo A. Stress relaxation function of bone and bone collagen. J Biomech. 1993; 26:1369–1376. [PubMed: 8308042]

51. Bowman SM, Gibson LJ, Hayes WC, McMahon TA. Results from demineralized bone creep tests suggest that collagen is responsible for the creep behavior of bone. J Biomech Eng. 1999; 121:253–258. [PubMed: 10211462]

52. Sasaki N, Nozoe T, Nishihara R, Fukui A. Effect of mineral dissolution from bone specimens on the viscoelastic properties of cortical bone. J Biomech. 2008; 41:3511–3514. [PubMed: 18996531]

53. Pathak S, Swadener JG, Kalidindi SR, Courtland HW, Jepsen KJ, Goldman HM. Measuring the dynamic mechanical response of hydrated mouse bone by nanoindentation. J Mech Behav Biomed Mater. 2011; 4:34–43. [PubMed: 21094478]

Highlights

- Effect of estrogen deficiency on the creep behavior of vertebral bone was examined.
- Correlations of creep parameters with bone mineral density, tissue mineral density and architectural parameters of vertebral bone were tested.
- Viscoelastic creep of vertebral bone under physiological loading was not fully recovered during the post-creep unloading period.
- A strong positive correlation was found between loading creep and residual displacement.
- Variability of tissue mineral density was the parameter that best determined creep parameters of estrogen deficient vertebrae.

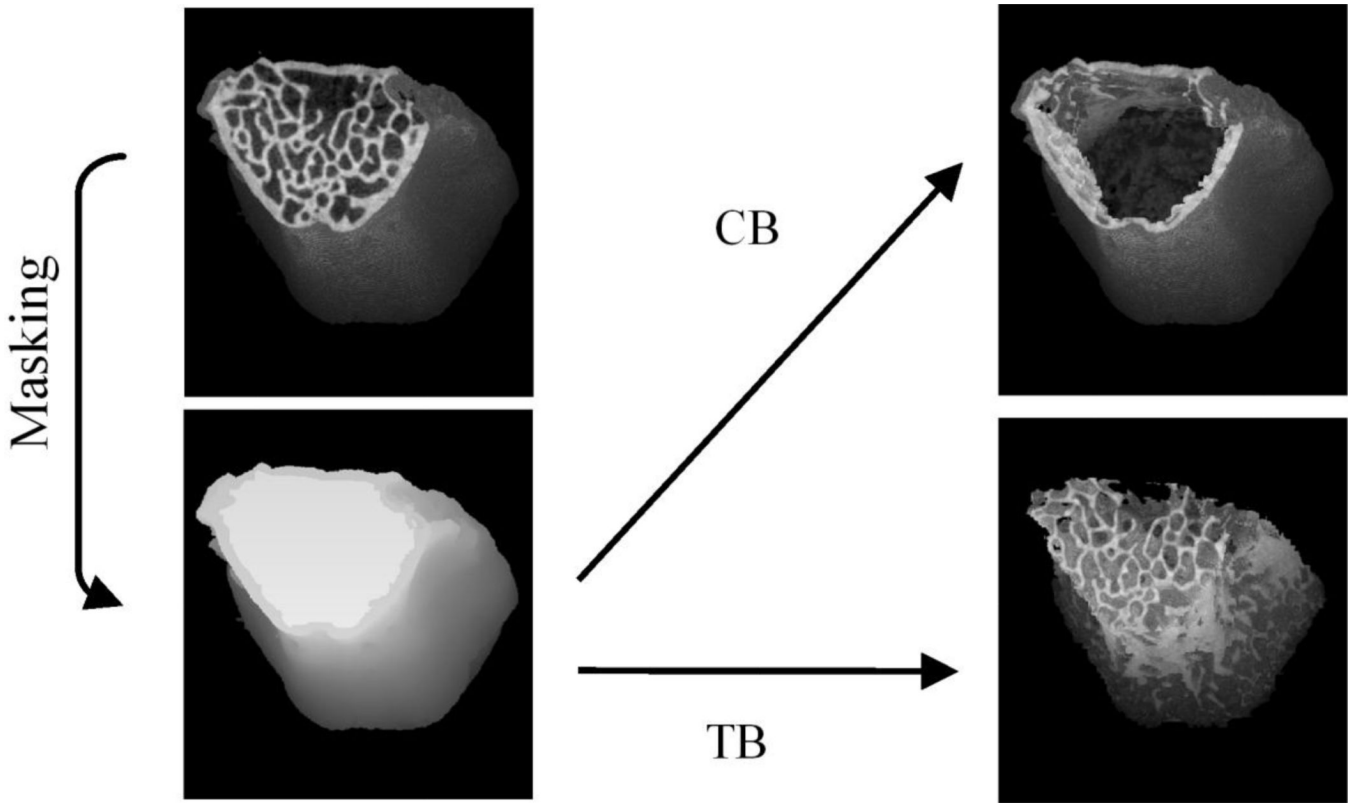

Fig. 1.

The procedure used to identify the vertebral centrum (Centrum) in masking region, the trabecular bone (TB) in the centrum, and the cortex (CB). In this figure, the endplate of the vertebra was digitally removed to show the trabecular centrum inside the vertebra, while the whole vertebral body was included in the analysis.

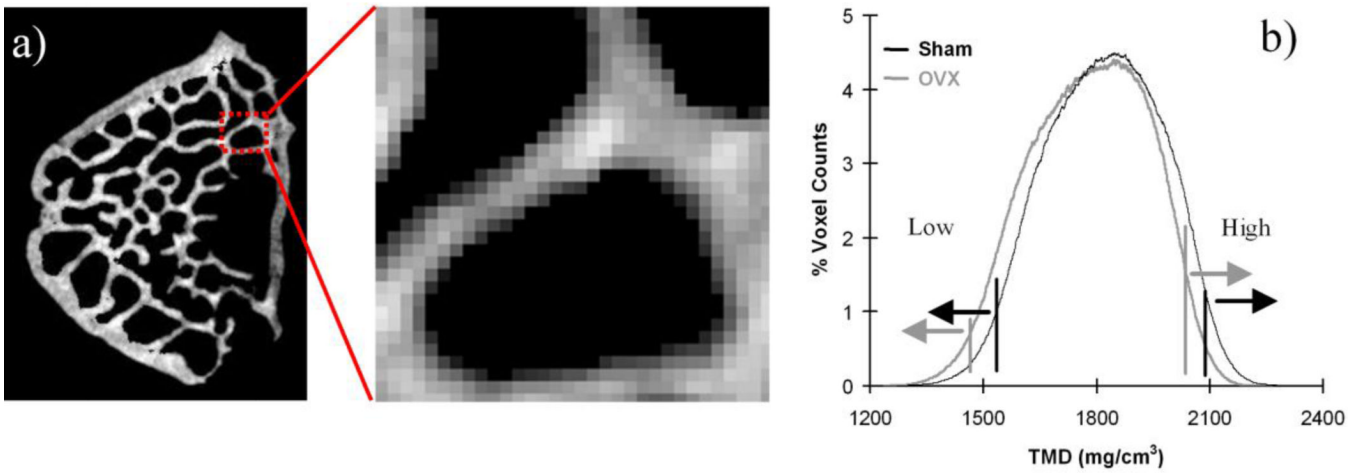

Fig. 2.

a) Detailed TMD distribution in TB. A darker color represents less TMD. b) A typical TMD histogram of a micro-CT image. The TMD distribution was different between the sham (black) and OVX (gray) groups.

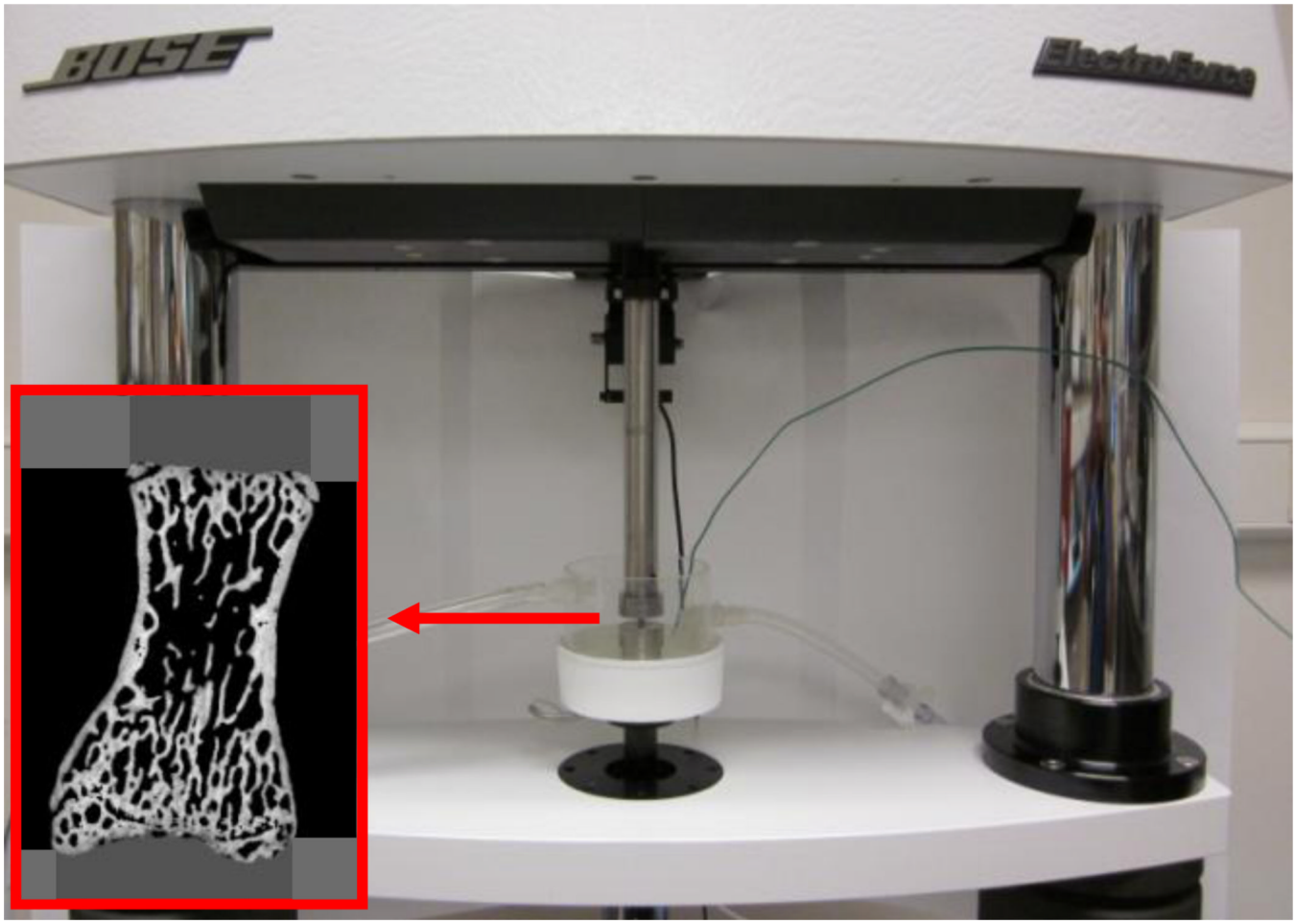

Fig. 3.
Loading machine with the environmental chamber and a specimen secured with dental cement.

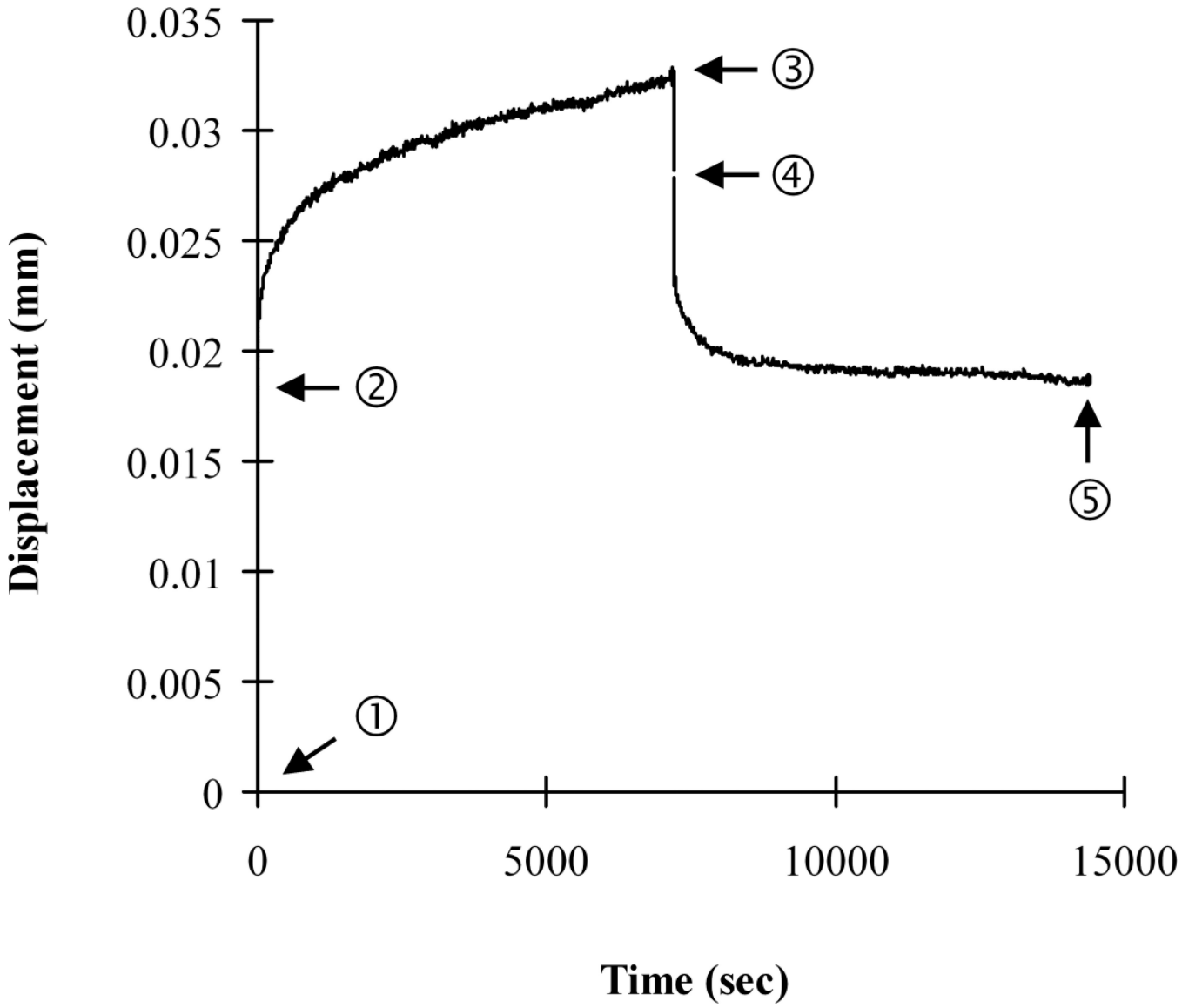

Fig. 4.

A typical displacement-time creep curve. Creep developed with time during loading (7200 sec) and unloading (7200 sec) periods. The terms related to mechanical creep testing were defined using the typical creep curves. ①; loading origin, ②-①; static loading displacement (d_l), ③-②; loading creep (C_l), ④-③; static unloading displacement (d_{ul}), ⑤-④; unloading creep recovery (C_{ul}), and ⑤; residual displacement (d_{res}).

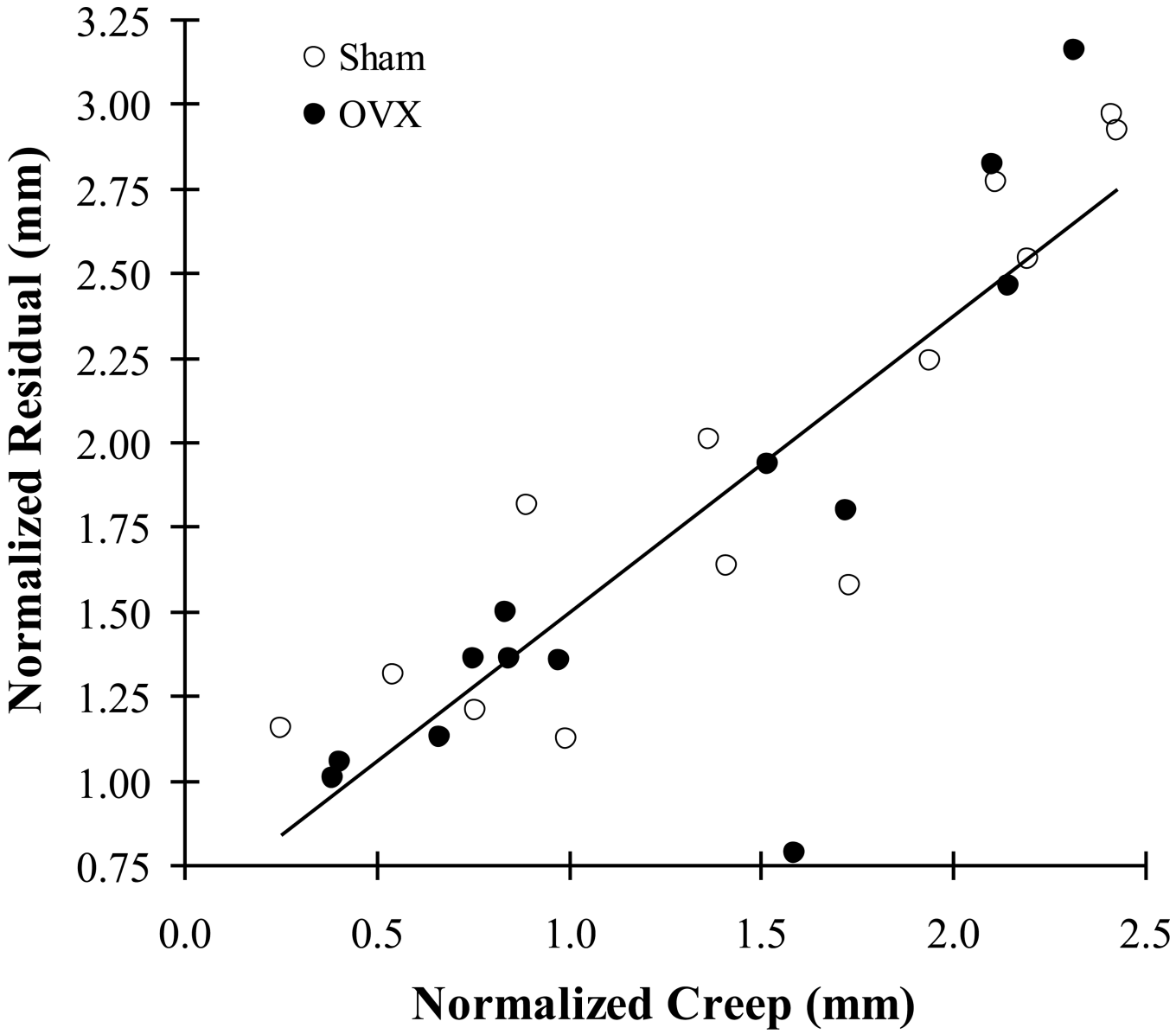

Fig. 5.
A strong positive correlation between normalized creep (C_l/d_l) and residual displacement (d_{res}/d_l) for both groups (r=0.868, p<0.001 for pooled group, n=26).

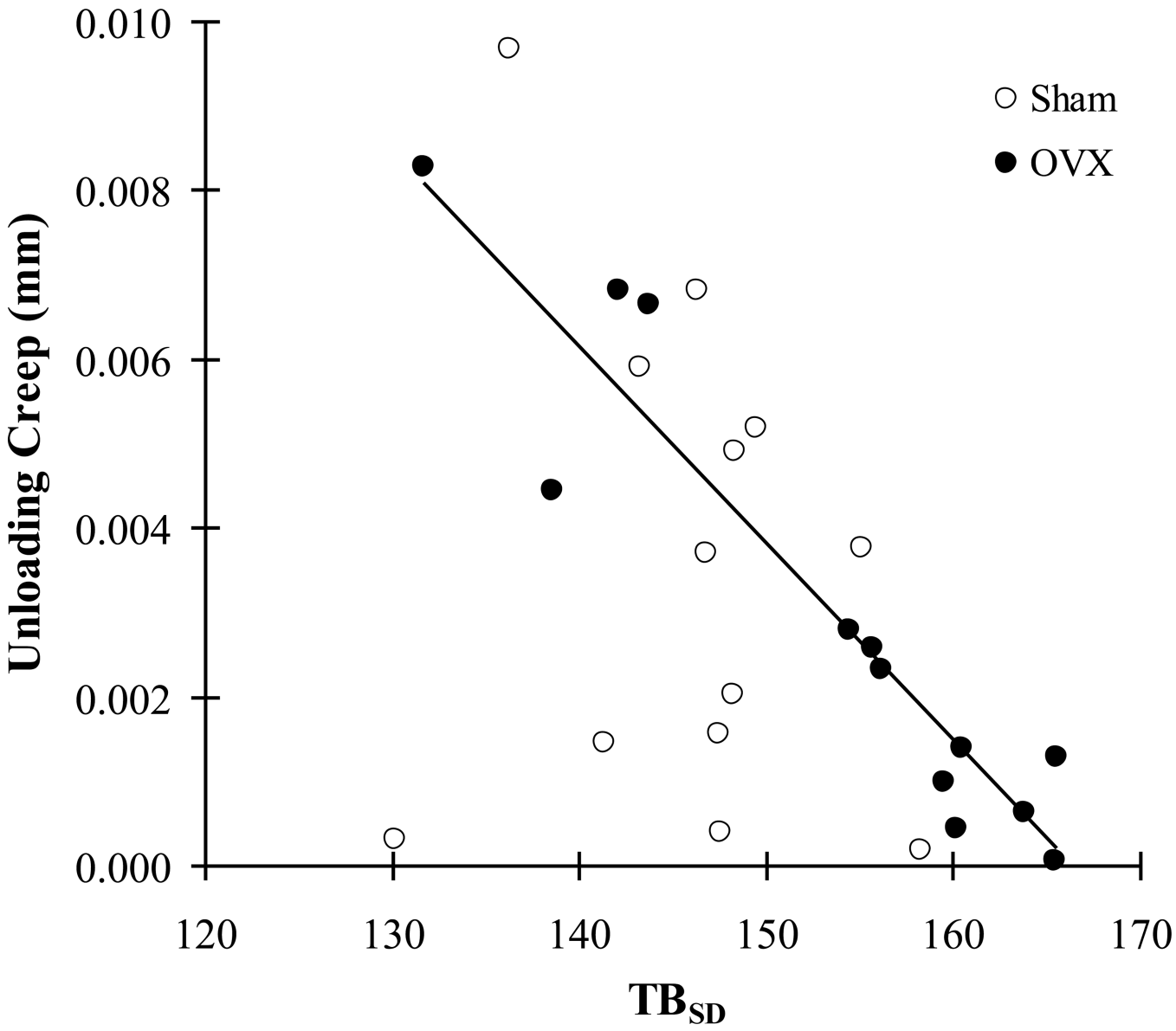

Fig. 6.

A correlation between unloading creep recovery (C_{ul}) and variability of trabecular tissue mineral density (TB_{SD}). The TB_{SD} of the OVX group has a significant, strong negative correlation with the unloading creep ($r=-0.942$, $p<0.001$, $n=13$), while that of the sham group does not have a significant correlation ($p=0.563$, $n=13$).

Table 1

Comparison of parameters between the sham (n=13) and OVX (n=13) groups. Significantly different ($p<0.05$) parameters are highlighted in bold.

Parameters		sham (mean±SD)	OVX (mean±SD)	p
TB BMD parameter	**BMD (mg/cm^3)**	**847.29±98.19**	**718.35±53.27**	**<0.001**
TMD parameters	**TB_{mean} (mg/cm^3)**	**1819.0±45.4**	**1754.7±29.7**	**<0.001**
	TB_{SD} (mg/cm^3)	**146.03±7.30**	**153.61±11.02**	**<0.05**
	TB_{COV}	**0.080±0.003**	**0.088±0.006**	**<0.001**
	TB_{low} (mg/cm^3)	**1570.7±39.9**	**1499.4±28.7**	**<0.001**
	TB_{high} (mg/cm^3)	**2043.6±54.0**	**1998.0±38.5**	**<0.021**
	CB_{mean} (mg/cm^3)	**1777.4±32.2**	**1744.2±32.4**	**<0.016**
	CB_{SD} (mg/cm^3)	164.72±9.00	165.65±10.51	0.810
	CB_{COV} (mg/cm^3)	0.093±0.004	0.095±0.006	0.232
	CB_{low}(mg/cm^3)	**1466.2±14.5**	**1445.5±12.6**	**<0.001**
	CB_{high}(mg/cm^3)	2009.0±41.9	1992.7±41.9	0.331
TB architectural parameters	**BV/TV**	**0.465±0.045**	**0.409±0.026**	**<0.001**
	Tb.N (mm^{-3})	4.885±0.536	4.719±0.261	0.325
	Tb.Th (mm)	**0.079±0.004**	**0.073±0.004**	**<0.002**
	Tb.Sp (mm)	0.128±0.028	0.139±0.014	0.196
	BS/BV (mm^{-1})	**25.30±1.342**	**27.41±1.672**	**<0.002**
	Conn.D (mm^{-3})	51.85±8.205	56.76±8.198	0.140
Initial condition parameters	f_1 (N)	25.19±16.74	16.80±10.23	0.136
	d_1 (mm)	0.015±0.008	0.017±0.009	0.657
Creep parameters	C_1 (mm)	0.018±0.010	0.017±0.007	0.703
	C_{ul} (mm)	0.004±0.003	0.003±0.003	0.619
	d_{res} (mm)	0.027±0.012	0.025±0.011	0.775
Normalized Creep Parameters	C_1/d_1	1.463±0.733	1.249±0.678	0.449
	C_{ul}/d_1	0.246±0.194	0.164±0.099	0.187
	d_{res}/d_1	1.945±0.684	1.672±0.734	0.336

Table 2

The parameters of the stepwise regression models that best explain creep (loading creep (C_l), unloading creep recovery (C_{ul}), residual displacement (d_{res})) and normalized creep, with applied displacement (d_l) (C_l/d_l, C_{ul}/d_l, d_{res}/d_l) parameters for each group and their correlations. A negative correlation coefficient (−r) indicates an inverse correlation.

		Creep Parameters			Normalized Creep Parameters		
		C_l	C_{ul}	d_{res}	C_l/d_l	C_{ul}/d_l	d_{res}/d_l
sham	Best Parameter	BV/TV	None	None	BMD	None	CB_{low}
	r	0.734	-	-	0.739	-	0.568
	p	0.05	-	-	<0.004	-	<0.043
OVX	Best Parameter	None	TB_{SD}	None	TB_{SD}	TB_{COV}	TB_{COV}
	r	-	−0.942	-	0.652	−0.625	0.580
	p	-	<0.001	-	<0.016	<0.023	<0.038